Molecular Biology of the Cell
Vol. 14, 4896–4908, December 2003

The Annexin 2/S100A10 Complex Controls the Distribution of Transferrin Receptor-containing Recycling Endosomes

Nicole Zobiack,*† Ursula Rescher,*†‡ Carsten Ludwig,* Dagmar Zeuschner,§ and Volker Gerke*‡

*Institute for Medical Biochemistry, Center for Molecular Biology of Inflammation, D-48149 Münster, Germany; and §Department of Cell Biology, University Medical Center Utrecht, 3584 CX Utrecht, The Netherlands

Submitted June 11, 2003; Revised August 7, 2003; Accepted August 21, 2003
Monitoring Editor: Anthony Bretscher

The Ca^{2+}- and lipid-binding protein annexin 2, which resides in a tight heterotetrameric complex with the S100 protein S100A10 (p11), has been implicated in the structural organization and dynamics of endosomal membranes. To elucidate the function of annexin 2 and S100A10 in endosome organization and trafficking, we used RNA-mediated interference to specifically suppress annexin 2 and S100A10 expression. Down-regulation of both proteins perturbed the distribution of transferrin receptor- and rab11-positive recycling endosomes but did not affect uptake into sorting endosomes. The phenotype was highly specific and could be rescued by reexpression of the N-terminal annexin 2 domain or S100A10 in annexin 2- or S100A10-depleted cells, respectively. Whole-mount immunoelectron microscopy of the aberrantly localized recycling endosomes in annexin 2/S100A10 down-regulated cells revealed extensively bent tubules and an increased number of endosome-associated clathrin-positive buds. Despite these morphological alterations, the kinetics of transferrin uptake and recycling was not affected to a significant extent, indicating that the proper positioning of recycling endosomes is not a rate-limiting step in transferrin recycling. The phenotype generated by this transient loss-of-protein approach shows for the first time that the annexin 2/S100A10 complex functions in the intracellular positioning of recycling endosomes and that both subunits are required for this activity.

INTRODUCTION

Receptors and their bound ligands, which are internalized via clathrin coated pits, first enter peripheral sorting endosomes where they are sorted according to their different destinations. Whereas the bulk of dissociated ligands and nonrecycled receptors is targeted to late endosomes and finally lysosomes for degradation, some receptors such as the transferrin receptor (TfR) escape degradation and recycle back to the plasma membrane. Recycling transferrin receptors accumulate in a perinuclear subpopulation of endosomal structures termed recycling endosomes (Gruenberg and Maxfield, 1995), which typically are enriched in the small GTPase rab11 (Ullrich *et al*., 1996; Sheff *et al*., 1999; Sonnichsen *et al*., 2000). However, a direct route from sorting endosomes back to the plasma membrane has also been described and may account for a significant amount of recycled transferrin in some cell types (Hopkins *et al*., 1994; Daro *et al*., 1996; Mellman, 1996). Although the recycling of the transferrin receptor has been characterized in detail, molecular mechanisms involved in the regulation of receptor trafficking through the various early endosomal subpopulations and parameters governing the intracellular positioning of endosomal subdomains have remained elusive to a large extent.

Annexin 2 belongs to the annexin multigene family of proteins that are able to interact Ca^{2+} dependently with cellular membranes through a highly conserved membrane-binding module, the annexin core. Annexins cycle between the cytosol and a specific target membrane and they are thought to be involved in a number of membrane-related events (Gerke and Moss, 2002). These include coated pit budding and the formation of plasma membrane microdomains, which both seem to require annexin 6 (Kamal *et al*., 1998; Babiychuk and Draeger, 2000) and the formation of apical transport vesicles at the *trans*-Golgi network, which involves annexin 13b (Lafont *et al*., 1998). However, despite their well-characterized structural and biochemical properties information on the intracellular functions of annexins is very scarce, in part due to a lack of specific ways to down-regulate a given annexin without activating compensatory mechanisms or annexin expressions.

Unique properties of the annexins are mediated through their N-terminal domains preceding the protein cores. In annexin 2, this N-terminal domain harbors the binding site for a protein ligand, the S100 protein S100A10 (p11) (Johnsson *et al*., 1988) as well as a Ca^{2+}-independent and thus

Article published online ahead of print. Mol. Biol. Cell 10.1091/mbc.E03–06–0387. Article and publication date are available at www.molbiolcell.org/cgi/doi/10.1091/mbc.E03–06–0387.

† These authors contributed equally to this work.

‡Corresponding authors. E-mail addresses: gerke@uni-muenster.de, rescher@uni-muenster.de.

Abbreviations used: bTf, biotinylated transferrin; DiI-LDL, DiI-labeled low-density lipoprotein; HRP, horseradish peroxidase; HRP-Tf, horseradish peroxidase-transferrin; siRNA, small interfering RNA; TfR, transferrin receptor; TxTf, Texas Red-labeled transferrin.

annexin-atypical membrane binding site (Jost *et al*., 1997). Complex formation with S100A10 results in an annexin 2/S100A10 heteroteramer with altered biochemical properties (Powell and Glenney, 1987). Among other things, it is only the annexin 2/S100A10 complex and not monomeric annexin 2 that can aggregate membrane vesicles at submicromolar Ca^{2+} concentrations (Drust and Creutz, 1988) and that can form highly symmetric junctions between opposing membrane surfaces indicative of a membrane scaffolding function (Lambert *et al*., 1997). Within the cell, membrane-bound annexin 2 is found at the plasma membrane and on endosomal membranes. The endosome localization, which requires the N-terminal membrane binding site (Jost *et al*., 1997), is in line with the finding that the protein is transferred from donor to acceptor membranes in homotypic endosomal fusion assays (Emans *et al*., 1993). Moreover, expression of a trans-dominant annexin 2 mutant protein that causes intracellular aggregation of annexin 2 and S100A10 perturbs the peripheral localization of early endosomes in polarized epithelial cells (Harder and Gerke, 1993). However, apart from this more indirect evidence, a role of annexin 2 in endosome organization and/or certain endosomal trafficking events has not been substantiated by direct loss-of-function approaches so far. It has also remained unanswered whether a potential endosome-associated function of annexin 2 requires formation of the complex with S100A10.

To address these questions, we used double-stranded RNA-mediated interference specifically suppressing the expression of either annexin 2 or S100A10. We show that down-regulation of both subunits results in a perinuclear clustering and condensation of recycling endosomes containing internalized transferrin (Tf). The phenotype can be reversed by reexpression of S100A10 or the N-terminal domain of annexin 2, respectively. The clustered endosomes show an increased amount of clathrin associated with endosomal buds but are not excluded from recycling internalized transferrin in an efficient manner.

MATERIALS AND METHODS

Cell Culture, Expression Constructs, and RNA Interference

HeLa cells were cultured in DMEM supplemented with 10% fetal calf serum, 100 U/ml penicillin, 100 μg/ml streptomycin, and 2 mM L-glutamine at 37°C in a humidified atmosphere with 7% CO_2.

To construct PMNanx2-GFP, a cDNA fragment encoding amino acids 1–27 of human annexin 2 with amino acid replacements I6E and L7E, which disrupt S100A10 binding (Thiel *et al*., 1992) was cloned in frame into pEGFP-N3 (BD Biosciences Clontech, Palo Alto, CA). Human S100A10 fused N-terminally to enhanced yellow fluorescent protein (YFP) was generated as described previously (Zobiack *et al*., 2001). For transient transfection, cells were either grown on coverslips or on 35-mm dishes and transfected with Effectene (QIAGEN, Valenica, CA) according to the manufacturer's protocol.

RNA oligonucleotides with 2-nt (2′-deoxy)-thymidine 3′ overhangs were obtained from Dharmacon Research (Lafayette, CO). Several small interfering RNA (siRNA) duplexes derived from different regions of the target mRNAs were tested for efficient gene-silencing. An annexin 2-specific siRNA duplex corresponding to nucleotides 146–165 of the coding sequence showed no down-regulation at all and was therefore chosen as a negative control in most of the experiments, whereas the siRNA duplex corresponding to nucleotides 94–113 was the most efficient annexin 2-specific siRNA. The S100A10-specific siRNA corresponded to nucleotides 84–103 of the human coding sequence. For siRNA transfections cells were grown on coverslips or on 35-mm dishes for 1 d before transfection. Annealed siRNA duplexes (100 nM) were transfected using OligofectAMINE (Invitrogen, Carlsbad, CA) according to the manufacturer's instructions. Both siRNA-treated and control cells were grown for 48 h at 37°C and then processed for further analyses. For rescue experiments, cells were transfected 24 h after siRNA treatment with the PMNanx2-GFP or YFP-S100A10 expression plasmids and cultured for another 24 h before further analysis.

Internalization of Endocytic Tracers

For internalization of Texas Red-labeled human transferrin (TxTf; Molecular Probes, Eugene, OR) or DiI-conjugated low-density lipoprotein (DiI-LDL; Molecular Probes), cells grown on coverslips were first serum-starved for 30 min at 37°C and then incubated in internalization medium (IM; minimal essential medium, 20 mM HEPES, 0.8 mg/ml sodium bicarbonate, 1 mg/ml bovine serum albumin, pH 7.2) containing 30 μg/ml TxTf or 50 μg/ml DiI-LDL. Incubations were carried out as indicated. The cells were then washed with ice-cold phosphate-buffered saline (PBS), fixed with 4% paraformaldehyde, and analyzed by fluorescence microscopy.

Transferrin Recycling Measurements

Human iron-saturated transferrin was coupled to horseradish peroxidase (HRP-Tf) as described previously (Stoorvogel *et al*., 1988). Cells grown on 35-mm dishes were washed, serum-starved for 30 min at 37°C in IM containing 50 μM desferal (deferoxamine mesylate), and then incubated for 30 min at 16°C in IM containing 2.5 μg/ml HRP-Tf ± 200 μg/ml unconjugated transferrin to accumulate label in sorting endosomes. Cells were then placed on ice, washed extensively, and plasma membrane-bound transferrin was removed by acid wash (20 mM MES, pH 5.0, 130 mM NaCl, 2 mM $CaCl_2$). Incubation was then continued at 16°C for 30 min with or without 100 nM wortmannin (Sigma-Aldrich, St. Louis, MO). Subsequently, cells were shifted to 37°C for the indicated chase periods. The amount of released and remaining intracellular transferrin was quantified by measuring HRP activity in the cell culture supernatants and the lysed cells, respectively. Recycling of HRP-Tf was calculated from the ratio of enzymatic activity of released HRP in the incubation medium to total activity.

Antibodies and Fluorescence Microscopy

Antibodies used were the monoclonal anti-annexin 2 antibody HH7 recognizing only monomeric annexin 2 in immunofluorescence, the polyclonal anti-annexin 2 antibody msa419, which recognizes both free and S100A10-complexed annexin 2, the monoclonal anti-S100A10 antibody H21 or the polyclonal anti-annexin 1 antibody r656, respectively (Gerke and Weber, 1984; Osborn *et al*., 1988; Thiel *et al*., 1992; Seemann *et al*., 1996). The anti-clathrin antibody was a kind gift from E. Ungewickell (Hannover Medical School, Hannover, Germany). Antibodies directed against rab11 and TfR (H68.4) were obtained from Zymed Laboratories (South San Francisco, CA), the anti-early endosomal antigen 1 (EEA1) antibody was from BD Transduction Laboratories (Lexington, KY), and the anti-vimentin antibody was from Immunotech (Emeryville, CA). The monoclonal anti-LAMP-1 antibody H4A3 developed by J.T. August and J.E.K. Hildreth was obtained from the Developmental Studies Hybridoma Bank developed under the auspices of the National Institute of Child Health and Human Development and maintained by the Department of Biological Sciences (University of Iowa, Iowa City, IA).

For immunofluorescence staining, fixed cells were permeabilized with 0.2% Triton X-100, quenched with 50 mM NH_4Cl in PBS, incubated with primary antibodies for 45 min, washed, and then incubated with the appropriate labeled secondary antibodies for 45 min. Coverslips were mounted in Mowiol (Aventis, Strasbourg, France). Images were acquired using a cooled charge-coupled device camera (Micromax; Princeton Scientific Instruments, Monmouth Junction, NJ) installed on a DM RXA fluorescence microscope (Leica, Wetzlar, Germany) or on an LSM510 Meta confocal microscope (Carl Zeiss, Jena, Germany).

Fractionation of Endosomal Membranes and Immunoblotting

Subcellular fractionation was carried out as described previously (Gorvel *et al*., 1991; Aniento *et al*., 1996). Briefly, cells were serum-starved for 30 min and then incubated in IM with 5 μg/ml biotinylated transferrin (bTf; Sigma-Aldrich) for 30 min at 16°C. After removing remaining plasma membrane-bound bTf by acid wash, cells were chased for 20 min at 37°C to preferentially label recycling endosomes. Cells were then homogenized in homogenization buffer (3 mM imidazole-HCl, pH 7.4, 0.25 M sucrose). Membrane fractions of the postnuclear supernatant were separated in a discontinuous sucrose flotation gradient and fractions enriched in early endosomes, late endosomes, and heavy membranes, respectively, were collected at the respective interfaces. Protein concentrations were measured with the Bradford assay (Perbio, Bonn, Germany) and aliquots were precipitated with trichloroacetic acid.

Proteins present in the total cell lysates or flotation gradient fractions were subjected to SDS-PAGE, transferred onto polyvinylidene difluoride membrane, and analyzed by immunoblotting with the antibodies specified. Internalized biotinylated transferrin was visualized using streptavidine conjugated to HRP (Sigma-Aldrich). Signal detection used enhanced chemiluminescence (Amersham Biosciences, Piscataway, NJ) according to the manufacturer's instructions. Signal intensities of the immune-reactive bands were measured using a Lumi-Imager (Roche Diagnostics, Mannheim, IN). The lysate blots shown are typical results of at least six individual transfections. Mean values ± SEM were calculated, and the statistical significance of the results was evaluated by unpaired *t* tests (*$p < 0.05$).

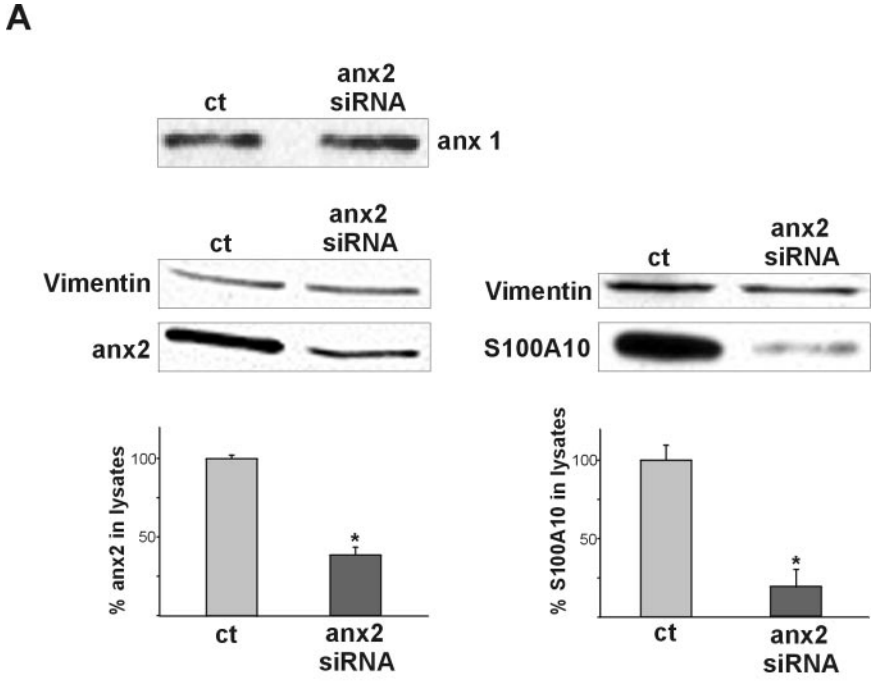

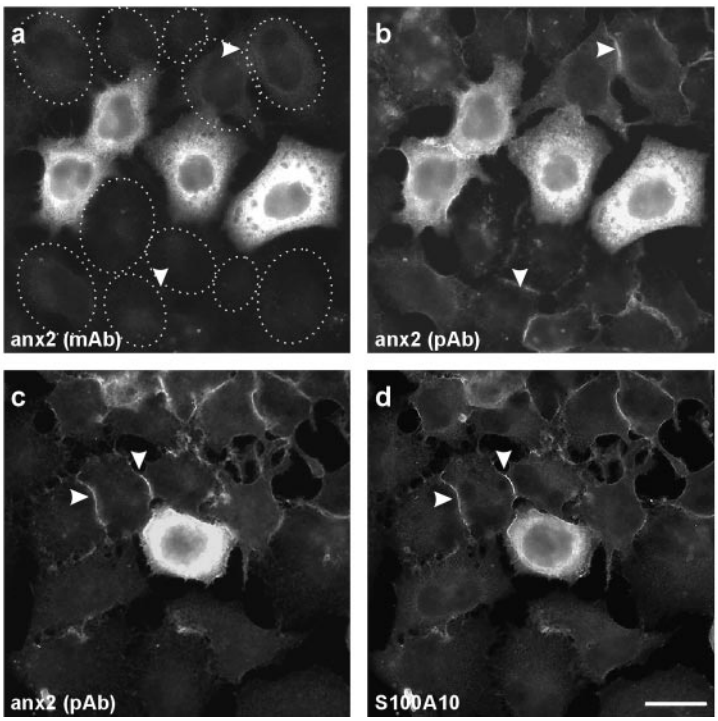

Figure 1. Protein levels and intracellular localization of annexin 2 and its cellular ligand S00A10 in HeLa cells transfected with annexin 2-specific siRNAi. (A) Immunoblot showing the protein amounts of annexin 1, annexin 2, vimentin, and S100A10 in HeLa cells lysates prepared from cells transfected with annexin 2-specific siRNA (anx2siRNA) or mock transfected control cells (ct). Note that annexin 1 expression was not altered, indicating the specificity of annexin 2 silencing. Vimentin served as an internal control for equal loading. A quantification of the annexin 2 and S100A10 signals determined by densitometry and calculated from at least six independent transfections is given below the blots. *$p < 0.05$. (B) Immunofluorescence staining of cells treated with annexin 2-specific siRNA using a monoclonal antibody (mAb) recognizing only free annexin 2 (a), polyclonal antibodies (pAb) recognizing both free and complexed annexin 2 (b and c), or an mAb recognizing the annexin 2 ligand S100A10 (d) revealed a strong decrease in annexin 2 and S100A10 expression, with only the cortical heterotetrameric annexin 2/S100A10 complex still detectable (arrowheads). Dotted lines indicate position of cells with reduced annexin 2 levels. Bar, 10 μm.

Whole-Mount Electron Microscopy

Whole-mount electron microscopy was performed as described previously (Zeuschner *et al*., 2001) with minor modifications. Cells were cultured on Formvar-coated golden grids and labeled for 5 min at 37°C in IM with 25 μg/ml HRP-Tf followed by a 20-min chase in IM containing 5 mg/ml HRP. Cells were incubated for 30 min on ice in 1.5 mg/ml 3–3′-diaminobenzidine tetrahydrochloride (DAB), 70 mM NaCl, 50 mM ascorbic acid, 20 mM HEPES, pH 7.2, supplemented with 0.02% H_2O_2 before use. The samples were washed in cold PBS and permeabilized for 30 min in PBS, pH 7.2, containing 1 mg/ml saponin, 5 mM ascorbic acid, 10 mM EGTA, 8.3 mM $CaCl_2$, 0.5 mg/ml $MgCl_2$, at 0°C. Subsequently, the grids were washed once with PBS containing 10 mM EGTA, 8.3 mM $CaCl_2$, 0.5 mg/ml $MgCl_2$ at 0°C and fixed in 2% paraformaldehyde, 0.2% glutaraldehyde in 0.1 M phosphate buffer, pH 7.4, for 1 h on ice. After three PBS washes at room temperature, free reactive aldehydes were quenched for 30 min in PBS, 50 mM NH_4Cl. Subsequently, the grids were transferred to blocking buffer (PBS containing 1 mg/ml saponin, 20 mM

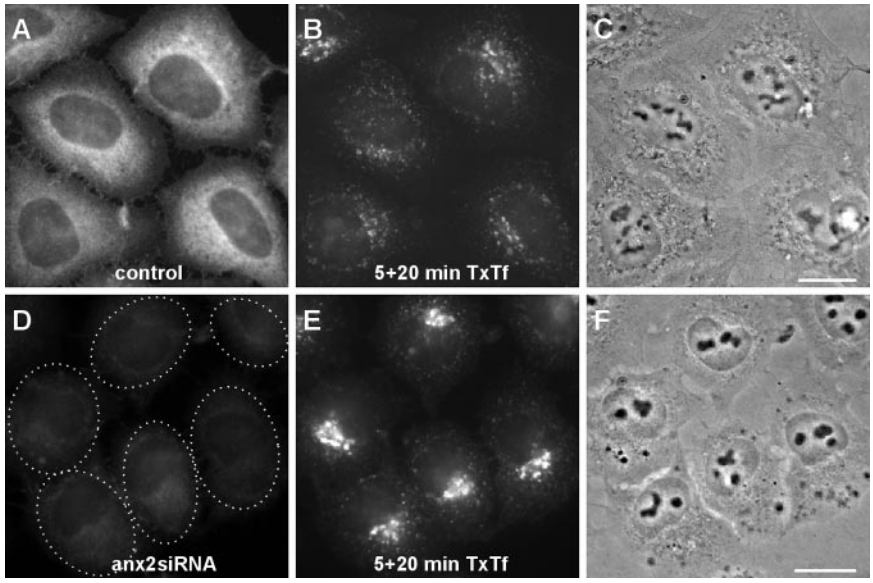

Figure 2. Annexin 2 gene-silencing specifically alters the distribution of transferrin-positive recycling endosomes. HeLa cells either mock-transfected (A and B) or transfected with annexin 2-specific siRNA (C and D) were incubated with TxTf at 37°C for 5 min followed by a 20-min chase to label the recycling endosomes. The annexin 2 distribution visualized by staining with the monoclonal HH7 antibody is given in A and D, whereas B and E show the distribution of internalized TxTf. Phase contrast images of the same cells are shown in C and F to visualize the localization of the nuclei. Note the marked perinuclear clustering transferrin label in the siRNA-treated cells. Bars, 10 μm.

glycine, 0.1% cold water fish gelatin, 0.02% NaN_3) and processed for double-immunogold labeling. The samples were dried using a critical point-drying apparatus (Balzers, Liechtenstein) and then stabilized with carbon film on top of the grids. They were examined and photographed in a JEOL transmission electron microscope at 80 kV. For quantification of immunogold labeling, nine areas showing comparable membrane structures in both siRNA-treated and control cells were selected from 3 individual micrographs and the respective gold labeling for transferrin receptor and clathrin was counted.

RESULTS

siRNA-mediated Down-Regulation of Annexin 2 Results in a Perinuclear Clustering of Internalized Transferrin

To study through a direct loss-of-function approach the involvement of annexin 2 in endocytosis, we aimed to reduce the expression of endogenous annexin 2 by using RNA interference. Immunoblot analysis as well as immunofluorescence revealed that transfection of the siRNA duplex targeted to nucleotides 94–113 of the human annexin 2 cDNA sequence led to a marked reduction (62%, on average) in the amount of endogenous annexin 2 after 48 h (Figure 1, A and B). Expression of an unrelated gene product, vimentin, or the closely related annexin 1 was not affected in the annexin 2 siRNA-treated cells, showing the specificity of the silencing (Figure 1A). Immunofluorescence analysis revealed a basically complete depletion of cytoplasmic and endosome-associated annexin 2 in the transfected cells (Figure 1B, a and b). With a polyclonal anti-annexin 2 antibody, some residual protein located at the plasma membrane could be identified (Figure 1B, b). This fraction most likely resembles annexin 2/S100A10 complexes that are stably incorporated into the cortical cytoskeleton, and, due to a masked epitope, are not detected by the monoclonal anti-annexin 2 antibody (Thiel *et al*., 1992). As judged by immunofluorescence, ~80–90% of the cells routinely show the annexin 2 depletion in our transient transfection approaches.

We next examined whether the down-regulation of annexin 2 by siRNA also affected the expression of the cellular ligand of annexin 2, S100A10. As shown in Figure 1A and B, c and d), a reduced annexin 2 level also resulted in a strongly decreased amount of S100A10 (reduction of 77% on average), most likely due to a limited stability of the free, non-complexed S100A10 protein (Puisieux *et al*., 1996). Because double labeling of annexin 2 and S100A10 in the siRNA-transfected cells showed an identical plasma membrane staining, the remaining S100A10 most likely resided in a complex with the remaining plasma membrane-associated annexin 2 (Figure 1B, c and d).

Endocytosis in the annexin 2/S100A10 down-regulated cells was analyzed by following the fate of several markers of distinct endocytic pathways. We first examined the distribution of TxTf in cells that had been pulsed for 5 min followed by a chase period of 20 min. In control cells, this pulse-chase procedure allowed most of the internalized transferrin to recycle out of the cell (see also below) with the remaining intracellular TxTf label associated with smaller structures dispersed throughout most of the cell (Figure 2 B). Strikingly, in annexin 2/S100A10 down-regulated cells, the TxTf fluorescence signal was much more concentrated in larger structures in the perinuclear region (Figure 2E). This aberrant TxTf accumulation was not due to a complete exit block, because the labeled transferrin could leave the cells after longer chase times of 40–60 min (our unpublished data). As shown in Figure 3A (top), the TxTf clusters observed in annexin 2/S100A10-depleted cells labeled with anti-rab11 antibodies, established markers for recycling endosomes.

We next examined whether decreasing annexin 2/S100A10 levels also perturbed structures in the late endocytic pathway. Therefore, we followed the internalization of labeled LDL, which dissociates from its receptor in sorting endosomes and is delivered to the late endosomal pathway. Double-labeling with the late endosome/lysosome marker LAMP-1 revealed that LDL internalized into annexin 2/S100A10-depleted cells is delivered to LAMP-1–positive structures, similar to those observed in mock-transfected cells (Figure 3A, bottom). Moreover, we could not observe any obvious differences in the uptake or transport of other lysosomal tracers in annexin 2/S100A10 down-regulated cells compared with control cells, e.g., labeled enhanced green fluorescent, or labeled bovine serum albumin, which is taken up by fluid phase endocytosis (our unpublished data).

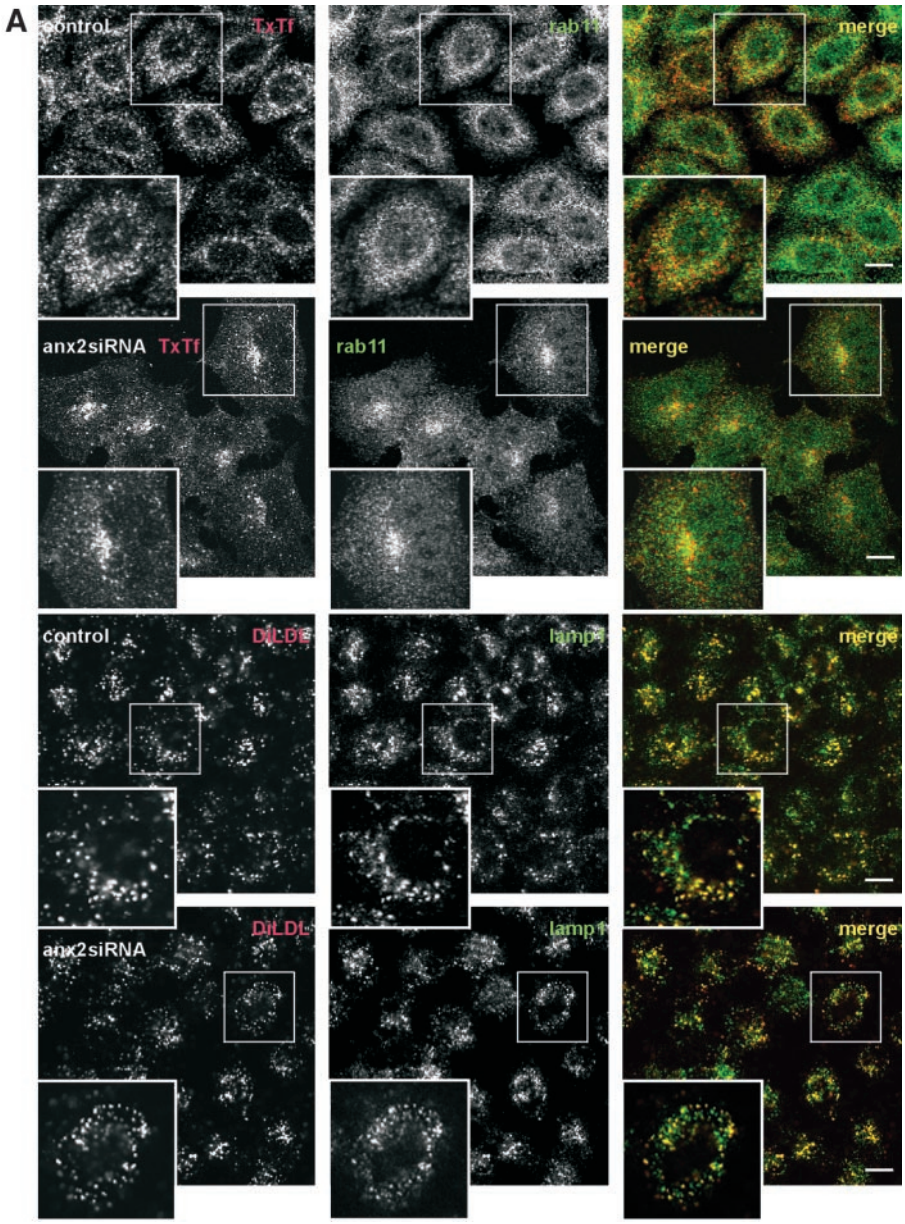

Figure 3. Down-regulation of annexin 2/S100A10 does not affect the internalization into sorting endosomes or transport along the late endocytic pathway. (A, top) HeLa cells were transfected with the annexin 2 siRNA (panels labeled anx2siRNA) or mock transfected (panels labeled control). To preferentially label recycling endosomes, cells were then allowed to internalize TxTf at 37°C for 5 min followed by 20-min chase. Distribution of rab11 (green label) was visualized using polyclonal anti-rab11 antibodies and merged with the localization of the labeled transferrin (red label). In cells with reduced annexin 2 levels, internalized TxTf accumulates in perinuclear rab11-positive structures. (A, bottom) Mock-transfected (control) or annexin 2 siRNA-transfected cells (anx2siRNA) were subjected to a 10-min pulse, 15-min chase procedure by using DiI-LDL (red label). Cells were then stained for LAMP-1 (green label) to confirm that late endosomes were labeled by the internalized DiI-LDL. No obvious differences in the distribution of DiI-LDL were observed in annexin 2 down-regulated compared with control cells. (B, top) TxTf was internalized into mock-transfected (control) or annexin 2-depleted cells (anx2siRNA) at 16°C for 30 min to label only sorting endosomes. These sorting endosomes did not accumulate in the perinuclear region of the annexin 2-silenced cells but showed a dispersed pattern identical to the distribution observed in control cells. A significant fraction of the TxTf-labeled sorting endosomes (red label) is positive for EEA1 as revealed by colabeling with monoclonal anti-EEA1 antibodies (green label). (B, bottom) Mock transfected (control) or siRNA-treated cells (anx2siRNA) were allowed to internalize TxTf at 16°C for 30 min and the distribution of rab11 (green label) was visualized in comparison with that of internalized TxTf (red label). Note some perinuclear accumulation of rab11 in the annexin 2-depleted cells. Bars, 10 μm. The enlarged insets show a twofold magnification of the boxed regions.

To clarify whether the perinuclear clusters containing TxTf and rab11, which were observed in annexin 2 down-regulated cells, were indeed recycling endosomes and not mislocalized sorting endosomes, we selectively loaded the sorting endosomes with transferrin at temperatures below 20°C. This treatment had been shown to prevent the transport of Tf from sorting to perinuclear recycling endosomes (Ren *et al*., 1998). In annexin 2/S100A10-silenced cells loaded at 16°C with TxTf, the label was now found in peripheral endosomes largely positive for the sorting endosome marker EEA1 (Figure 3B, top). It did not accumulate in the perinuclear area, although some perinuclear clustering of rab11 is also observed in cells kept at 16°C (Figure 3B, bottom). Thus, uptake and trafficking of transferrin to sorting endosomes are not affected in the siRNA-treated cells. This was also corroborated by quantifying the rate of internalization of HRP-conjugated Tf, which revealed no difference between control and annexin 2/S100A10 down-regulated cells (our unpublished data).

To investigate whether the striking perinuclear accumulation of internalized transferrin observed in annexin 2/S100A100 down-regulated cells alters the rate of transferrin recycling or the composition of TfR-positive endosomes, we performed a series of biochemical analyses. First, recycling rates were determined by allowing cells to endocytose HRP-conjugated transferrin for 30 min at 16°C and recording the reappearance of the internalized transferrin after different chase times by measuring HRP activity in the medium. Compared with the recycling in control cells, transfection with active annexin 2 siRNA caused no major changes in transferrin recycling (Figure 4 A). It should, however, be noted that the recycling rate was consistently reduced by a small value of ~5% in the down-regulated cells.

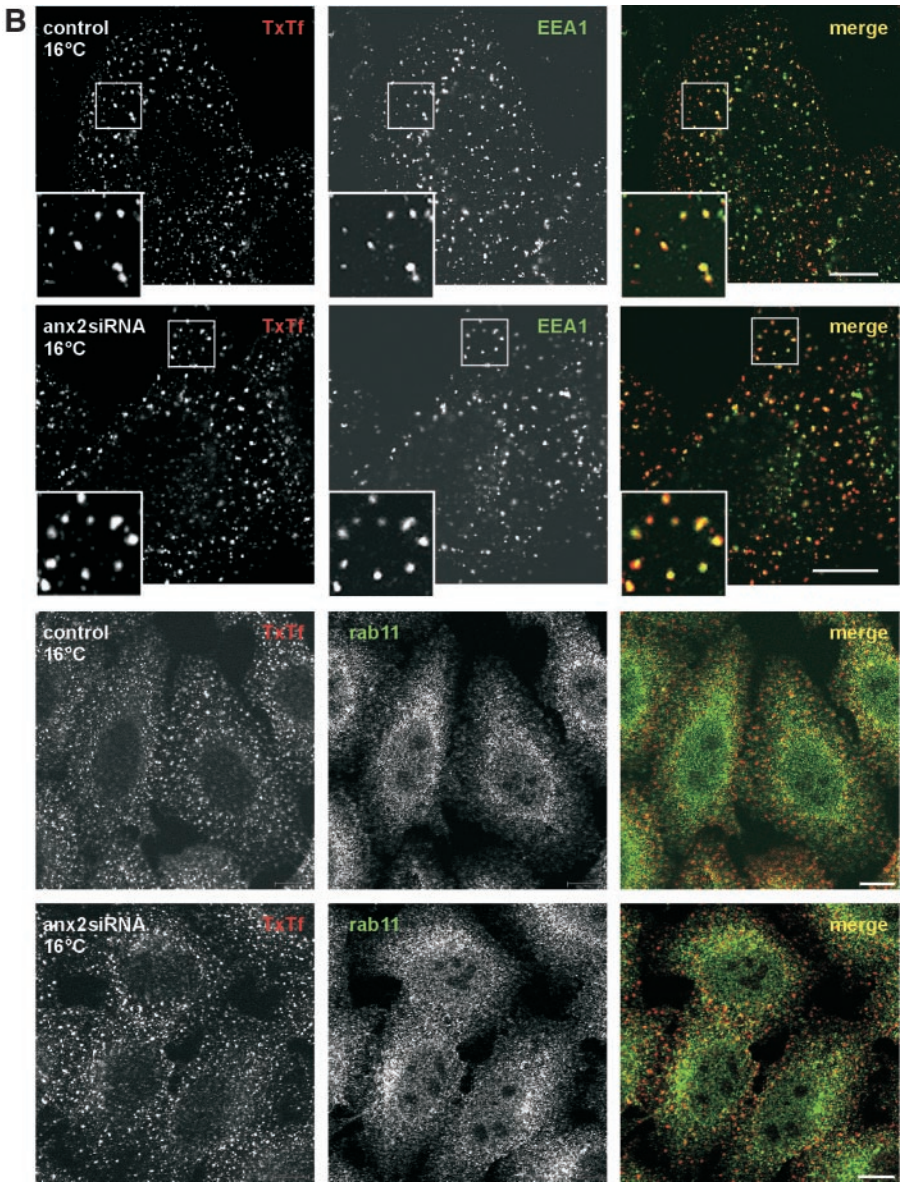

Figure 3 (cont)

At least two routes have been shown to mediate recycling of internalized transferrin receptors with only one of them involving the perinuclear recycling compartment (Sheff *et al*., 1999, 2002; van Dam and Stoorvogel, 2002). The second, more direct pathway can account for a substantial amount of recycling and may compensate for losses in recycling through the perinuclear endosomes. Because such compensatory mechanism could mask a potential inhibitory effect of annexin 2/S100A10 down-regulation on recycling involving perinuclear endosomes, we also measured the recycling rates in cells treated with wortmannin, a phosphatidylinositol 3-kinase inhibitor known to block the direct recycling from sorting endosomes (van Dam and Stoorvogel, 2002). Figure 4A reveals that wortmannin blocks the total recycling by ~20% in control cells. A similar reduction by wortmannin is seen in the annexin2 siRNA-transfected cells, indicating that annexin 2/S100A10 depletion does not up-regulate a wortmannin-sensitive recycling pathway. Thus, the rate of recycling internalized TxTf through wortmannin sensitive or insensitive pathways seems not to be affected by annexin 2 siRNA treatment. However, we cannot exclude that effects on recycling rates might become evident upon a more stringent depletion of annexin 2 because the level of down-regulation is ~60% in our experiments. However, the annexin 2/S100A10 remaining in our siRNA-treated cells is largely restricted to the subplasmalemmal region and thus unlikely to effect endosomal recycling.

To analyze whether the density of endosomal membranes and the profile of associated marker proteins is affected by annexin 2/S100A10 down-regulation, we performed discontinuous sucrose gradient fractionation of endosomal organelles. Cells were allowed to internalize bTf, and endosomal membranes present in a postnuclear supernatant prepared from these cells were separated in a sucrose step gradient (Gorvel *et al*., 1991). Internalized transferrin present in the endosomal membrane fractions was then detected using streptavidin, and its distribution over the gradient was compared with that of the EEA1 and the small GTPase

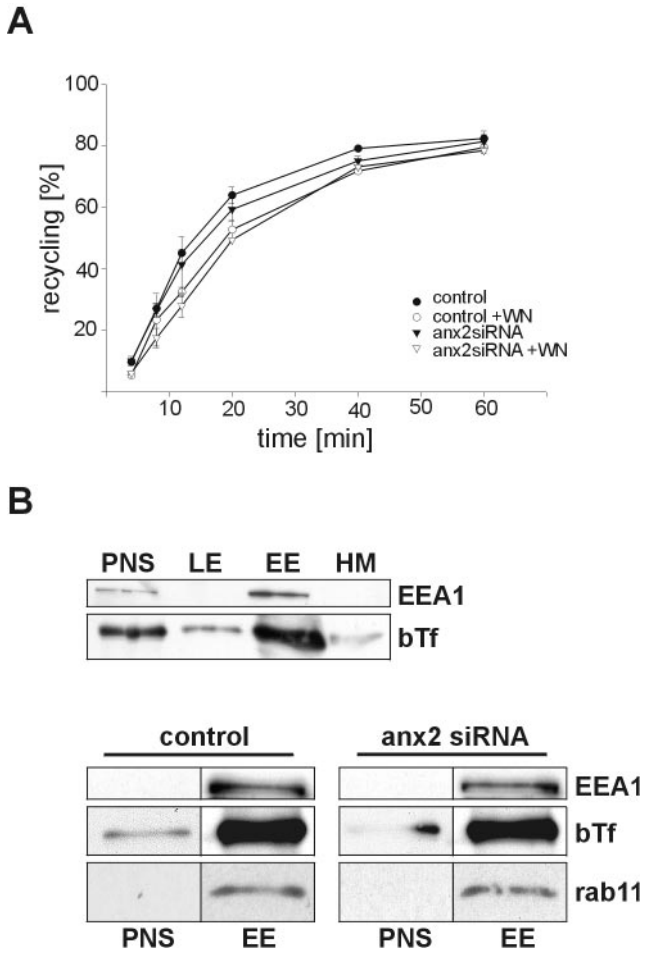

Figure 4. Analysis of transferrin recycling and endosomal membrane fractionation in annexin 2/S100A10 down-regulated cells. (A) Kinetics of transferrin recycling. Cells transfected with the annexin 2-specific siRNA (▼) or mock-transfected control cells (●) were incubated with HRP-Tf for 30 min at 16°C. After removing surface bound Tf by acid wash, cells were incubated in the presence (open symbols) or absence (closed symbols) of 100 nM wortmannin (WN), shifted to 37°C, and the release of recycled Tf was monitored at the indicated times by measuring released and remaining intracellular HRP enzymatic activity. Recycled Tf was calculated as percentage of released to total HRP activity. Each time point represents the mean of triplicate samples. The experiment was repeated three times with similar results, and a typical set of data is given. (B) Endosomal membranes and distribution of internalized transferrin. HeLa cells transfected with the annexin 2-specific siRNA or mock-transfected cells (control) were fed with biotinylated transferrin to preferentially label recycling endosomes and homogenized. Membrane fractions of the postnuclear supernatant (PNS) were separated in a discontinuous sucrose flotation gradient and fractions enriched in early endosomes (EE), late endosomes (LE), and heavy membranes (HM), respectively, were analyzed by SDS-PAGE and subsequent Western blotting. As shown in the top panel, internalized bTf is mainly recovered in the EEA1-positive fraction containing sorting and recycling endosomes. The bottom panels show the presence of internalized bTf, EEA1, and rab11 in fractions enriched in early, i.e., sorting and recycling, endosomes. No differences in these fractions from control compared with annexin 2/S100A10-depleted cells could be detected. LE and HM fractions were also analyzed in these experiments but not shown because no aberrant accumulation of EEA1, bTf, or rab11 was seen in these fractions. The subcellular fractionations indicate that the density and composition of recycling endosomes and the delivery of internalized transferrin to these structures is unaffected by annexin 2/S100A10 depletion.

rab11. The majority of bTf was recovered in the early endosome fraction containing sorting and recycling endosomes in both control and annexin 2/S100A10-depleted cells (Figure 4B). Thus, the overall density and composition of early/recycling endosomes and the delivery of internalized transferrin to these structures seem to be unaffected by annexin 2/S100A10 down-regulation.

siRNA-mediated Down-Regulation of S100A10 Alone Also Induces an Aberrant Localization of Recycling Endosomes

Because annexin 2-specific gene-silencing led to a concomitant reduction of S100A10, it was not possible to decide whether the observed effects on recycling endosome distribution were a consequence of the depletion of annexin 2, S100A10, or the annexin 2/S100A10 complex, respectively. To address this point, we selected siRNA duplexes to down-regulate S100A10 directly. As revealed by Western blot and immunofluorescence, S100A10 could be efficiently down-regulated with <19% of the protein remaining in the transfected cells (Figure 5A). This residual S100A10 is restricted to the subplasmalemmal region (our unpublished data) and thus most likely resides in the stable annexin 2/S100A10 complexes of the cell cortex, which are also resistant to annexin 2 siRNA treatment (see above; Figure 1). S100A10-specific down-regulation had no effect on the level of annexin 2 (Figure 5A). Thus, in contrast to noncomplexed S100A10, monomeric annexin 2 is stable within the cells.

Pulse-chase experiments using TxTf revealed that S100A10 depletion alone also led to an accumulation of internalized transferrin in perinuclear clusters (Figure 5B). The clusters were positive for rab11 (our unpublished data) and thus most likely resembled the aberrantly positioned recycling endosomes seen in annexin 2 siRNA-treated but not mock-transfected cells (Figure 2). Uptake of TxTf into sorting endosomes, the intracellular distribution of sorting endosomes, and the delivery of markers to the degradative pathway were not affected in the S100A10-depleted cells (our unpublished data). The recycling of internalized transferrin was also not significantly impaired, and wortmannin induced similar reduction rates in both control and S100A10-treated cells (Figure 5C). Thus, in our analyses of endosome distribution and endosomal transport, siRNA-mediated down-regulation of S100A10 has the same phenotypic consequences as depletion of the annexin 2/S100A10 complex mediated by annexin 2 siRNA treatment. Because annexin 2 protein levels remain unchanged in the S100A10 siRNA-transfected cells, we can conclude that monomeric annexin 2 is not sufficient to maintain the proper positioning of recycling endosomes.

The Ultrastructure of Recycling Endosomes in Annexin 2/S100A10 Down-regulated Cells

To examine whether the observed accumulation of transferrin in annexin 2/S100A10-depleted cells was due to changes in the ultrastructure of recycling endosomes, we analyzed the cells by whole-mount immunoelectron microscopy, a technique that has been used successfully to visualize morphological aberrations in recycling endosomes of cells expressing a dominant-negative dynamin^{-1} mutant (van Dam and Stoorvogel, 2002). Cells grown on grids were allowed to endocytose HRP-Tf for 5 min followed by a 20-min chase period. Cells were then placed at 0°C in a buffer containing DAB, which polymerizes in HRP-containing compartments. Cytosolic proteins were washed out after permeabilizing the cells with saponin and cells were immunogold-labeled with different antibodies and inspected by transmission electron microscopy. A first striking difference

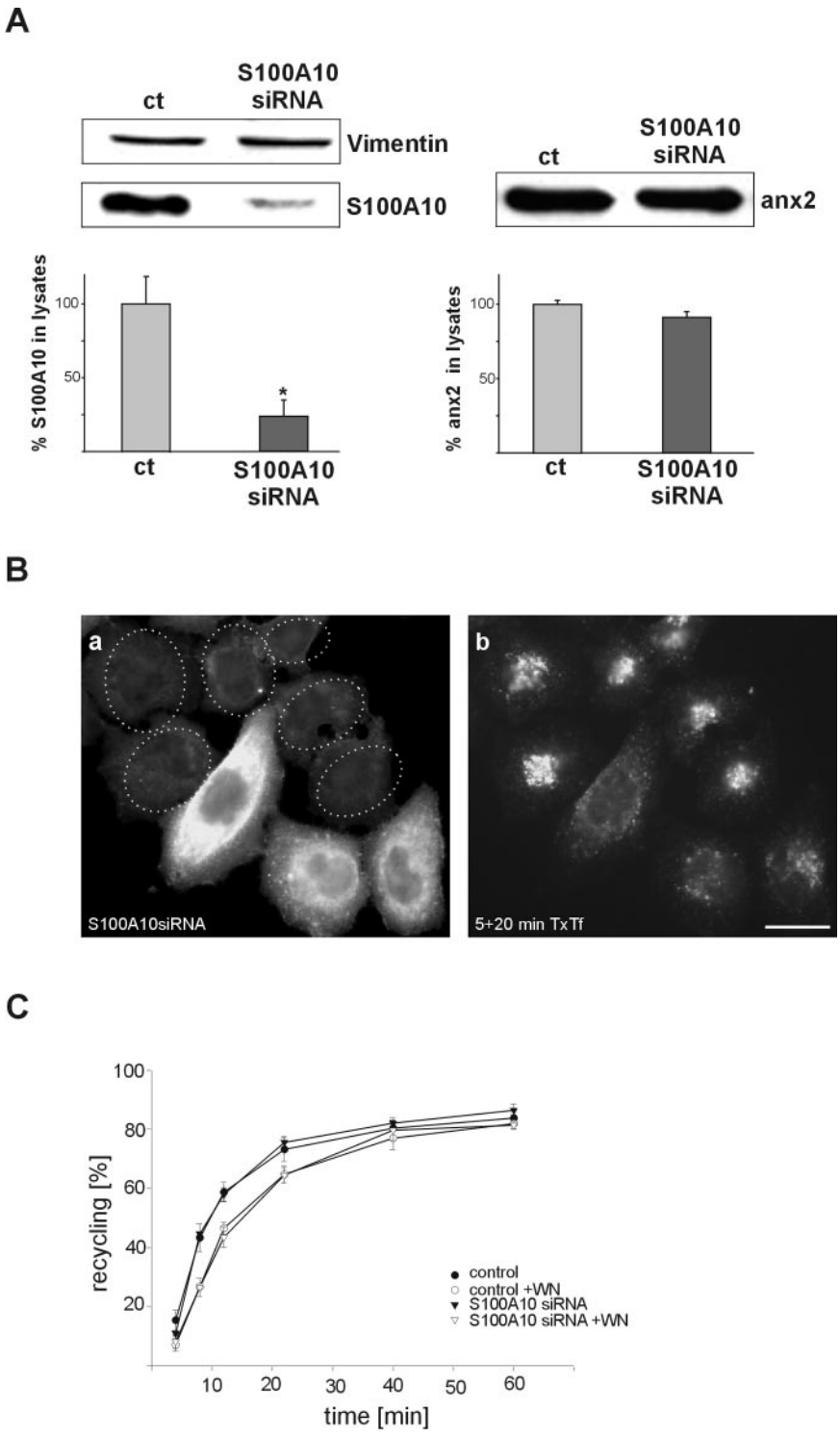

Figure 5. siRNA-mediated silencing of S100A10 specifically alters the positioning of transferrin receptor positive recycling compartment. (A) S100A10 and annexin 2 protein amounts were determined by immunoblotting of lysates prepared from S100A10siRNA-transfected cells. Whereas S100A10 expression is strongly decreased, annexin 2 protein level remains unchanged. Vimentin served as an internal control for equal loading. The corresponding bar graphs were calculated from the densitometric data of at least six independent transfections. *$p < 0.05$. (B) Immunofluorescence staining with anti-S100A10 antibodies confirmed the siRNA-mediated gene silencing of S100A10. Dotted lines indicate the position of cells with reduced S100A10 level (a). Pulse-chase labeling with TxTf revealed an accumulation of transferrin-positive perinuclear endosomes in cells with down-regulated S100A10 (b). Bar, 10 μm. (C) Kinetics of transferrin recycling. Cells transfected with the S100A10-specific siRNA (▼) or control cells (●) were incubated with HRP-Tf for 30 min at 16°C. After removing surface bound Tf by acid wash, cells were incubated in the presence (open symbols) or absence (closed symbols) of 100 nM wortmannin (WN), shifted to 37°C, and the release of recycled Tf was monitored at the indicated times by measuring released and remaining intracellular HRP enzymatic activity. Recycled Tf was calculated as percentage of released to total HRP activity. Each time point represents the mean of triplicate samples. The experiment was repeated three times with similar results, and a typical set of data is given.

between control cells and annexin 2/S100A10 down-regulated cells was already seen at low magnification. Whereas in control cells the recycling endosomes labeled by the pulse-chase procedure, i.e., structures looking dark due to the HRP-mediated DAB polymerization, were relatively spread out throughout the cell, more condensed recycling endosomes clustered in the perinuclear region were evident in the annexin 2/S100A10 down-regulated cells (Figure 6, A and B). Higher magnification revealed HRP-Tf positive endosomes as vacuolar-tubular structures positive for TfR and annexin 2 in control cells (Figure 6C). Consistent with the immunofluorescence analysis, no annexin 2 could be detected on endosomal structures in siRNA-transfected cells, which stained heavily for the TfR (Figure 6D). A closer inspection of the aberrantly positioned endosomes in the down-regulated cells showed that they often formed highly

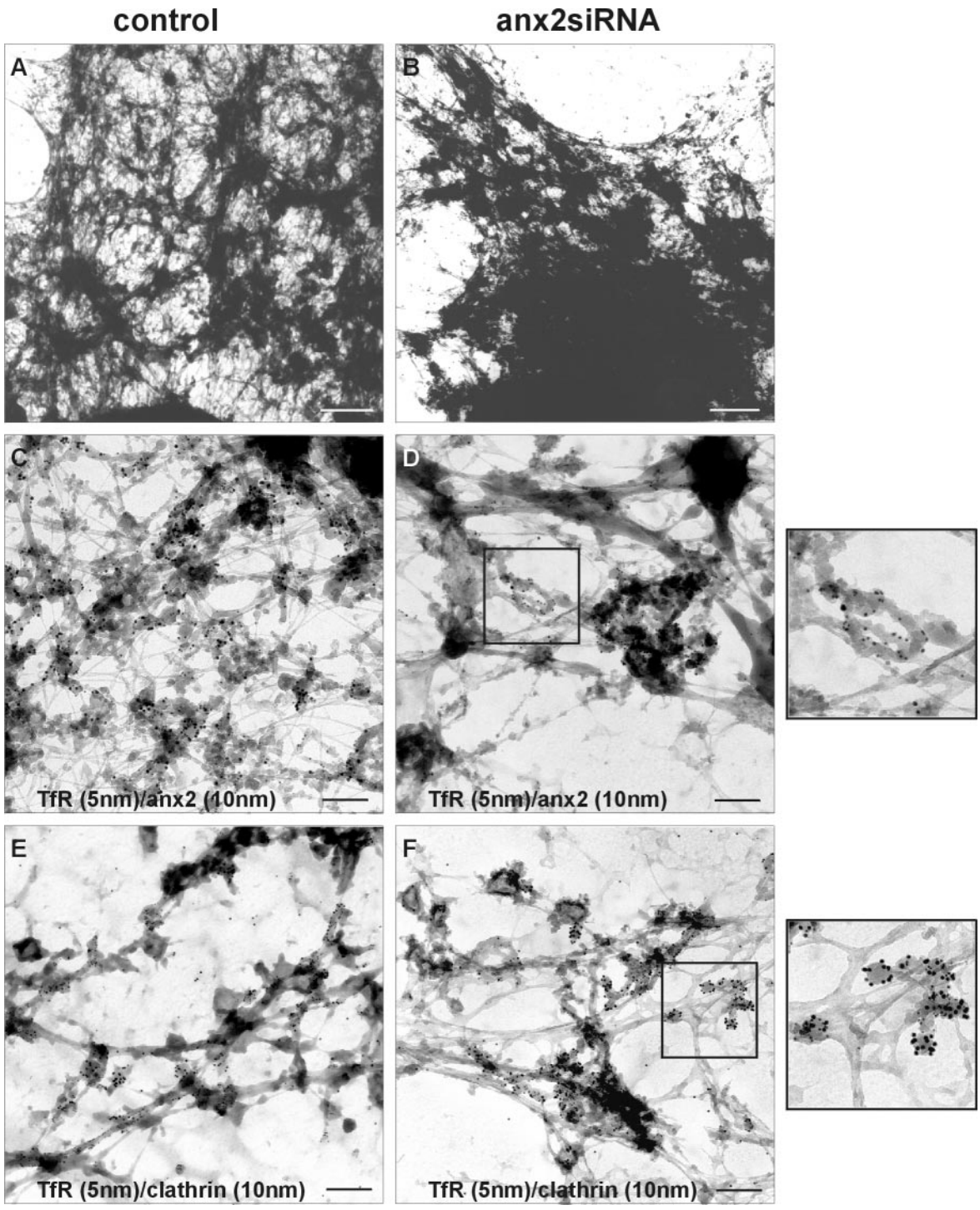

Figure 6. Ultrastructural analysis of endosomes in annexin 2 siRNA-treated cells. HeLa cells were either mock-transfected (control, A, C, and E) or transfected with annexin 2 siRNA (anx2siRNA, B, D, and F). Cells were then labeled by using a pulse-chase protocol to accumulate HRP-Tf in recycling endosomes and subsequent incubation with DAB that polymerizes in HRP-containing compartments. After permeabilization and immunogold labeling, the cells were inspected by transmission electron microscopy. Due to the HRP-Tf labeling/HRP pulse/DAB polymerization protocol only early, i.e., HRP-positive sorting and recycling endosomes look like dark structures in the electron micrographs. Low magnifications showing a part of the cell, excluding the nucleus, are given in A and B. Here, the labeled endosomes looked like tubular structures throughout the control cells (A), whereas they were more condensed and clustered in the perinuclear region in annexin 2/S100A10 down-regulated cells (B). Bars, 1 μm. Higher magnification of cells labeled with antibodies against TfR (C–F, 5-nm gold), annexin 2 (C and D, 10-nm gold), and clathrin (E and F, 10-nm gold). In control cells (C and E), annexin 2 (C, 10-nm gold) was found on tubular structures enriched in transferrin receptors (C, 5-nm gold). Clathrin (E, 10-nm gold) was associated with individual transferrin receptor (E, 5-nm gold)-positive buds along tubular membranes. In cells transfected with annexin 2-specific siRNA (D and F), no label of endosome-associated annexin 2 was detectable (D) with the few 10-nm gold particles visible representing background of the secondary antibody. The

bent tubules of almost circular shape (Figure 6D, inset). Such structures were not seen in control cells (Figure 6C). Moreover, an increased number of endosomal buds heavily decorated with clathrin was evident (Figure 6F). Because the amount of clathrin on these buds seemed to be significantly increased in cells depleted of annexin 2/S100A10, we quantified the ratio of clathrin versus TfR immunogold found on the endosomal buds. Although the ratio was 1:7 (clathrin: TfR) in control cells, it was increased to 1:2 in the depleted cells.

The Annexin 2-S100A10 Complex but Not S100A10 Per Se Is Required for the Proper Positioning of Recycling Endosomes

The above-mentioned analyses established a crucial role for S100A10 in maintaining a proper endosome distribution because direct down-regulation by S100A10 siRNA (Figure 5) as well as reduction of S100A10 levels via annexin 2 siRNA-mediated depletion of the complex partner annexin 2 (Figure 2) caused a perinuclear accumulation of recycling endosomes. However, the data could not distinguish between S100A10 alone or the heterotetrameric annexin 2/S100A10 complex being the functionally relevant component. To answer this question, we carried out a series of rescue experiments. First, we expressed YFP-tagged S100A10 previously shown to be capable of annexin 2/S100A10 complex formation (Zobiack *et al*., 2001) in S100A10- as well as annexin 2/S100A10-depleted cells. As revealed by YFP fluorescence (Figure 7, A and C) as well as Western blot analysis using anti-YFP/green fluorescent protein (GFP) antibodies (our unpublished data) the YFP-S100A10 derivative was expressed in both S100A10 as well as annexin 2/S100A10 down-regulated cells. The appearance of recycling endosomes was then again visualized by monitoring the signal of internalized TxTf chased for 20 min along the recycling pathway. Figure 7, A and B, reveals that the perinuclear clustering of TxTf induced by S100A10 depletion was reversed upon YFP-S100A10 expression with the label now occurring in recycling vesicles more widely spread throughout the cell. In contrast, recycling endosome clustering induced by annexin 2 down-regulation and concomitant S100A10 depletion remained unchanged upon expression of YFP-S100A10 (Figure 7, C and D). This strongly suggests that the annexin 2/S100A10 complex is the relevant unit required for recycling endosomes positioning.

Next, we attempted to reverse the phenotype in annexin 2/S100A10-depleted cells (transfected with the annexin 2 siRNA) by expressing the unique N-terminal domain of annexin 2. This N-terminal domain harbors the binding site for S100A10 (Johnsson *et al*., 1988) and also contains a nonoverlapping membrane binding site that enables the protein to interact with endosomal membranes in the absence of Ca^{2+} (Jost *et al*., 1997). The N-terminal domain, which had been mutated to render the S100A10 binding site inactive without affecting the endosome binding site (Jost *et al*., 1997), was expressed as a GFP fusion protein termed PMNanx2-

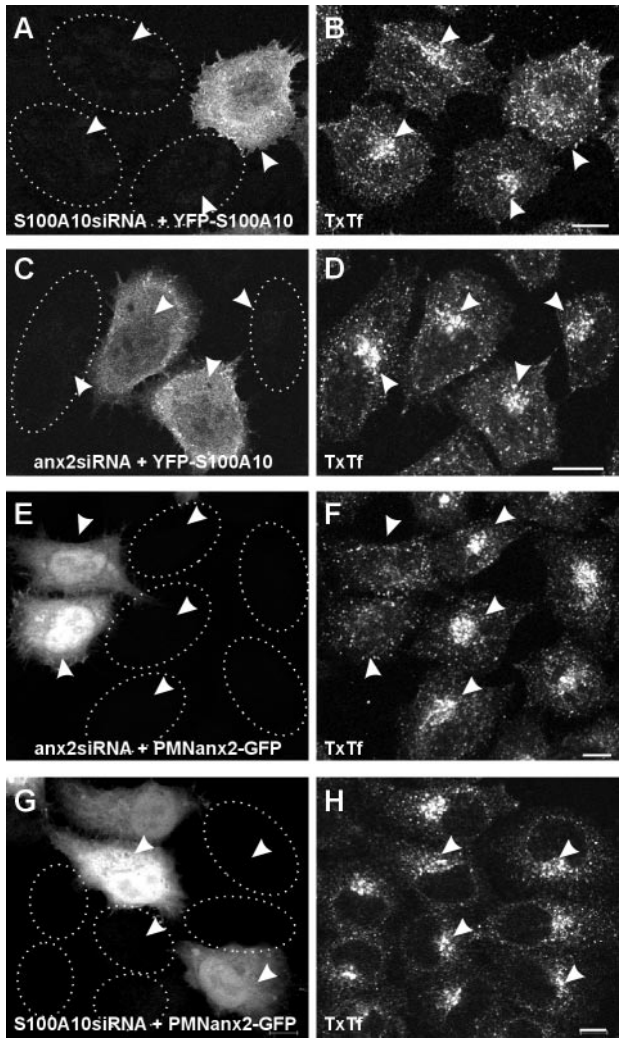

Figure 7. Expression of S100A10 or the N-terminal domain of annexin 2 rescues the S100A10 or annexin 2 siRNA phenotype, respectively. HeLa cells silenced and additionally transfected with expression plasmids indicated were pulsed for 5 min with TxTf followed by a 20-min chase. The intrinsic YFP and GFP fluorescence identifying YFP-S100A10– and PMNanx2-GFP–expressing cells is given in A, C, E, and G, respectively, whereas B, D, F, and H show the distribution of internalized TxTf. Although the characteristic clustering of the internalized transferrin was seen in S100A10-silenced cells (A and B), expression of YFP-S100A10 restored the phenotype with the label now occurring in vesicles more widely spread throughout the cell (A and B). In annexin 2 siRNA-treated cells depleted of the annexin 2/S100A10 complex, the perinuclear accumulation of TxTf in clustered recycling endosomes could not be rescued by YFP-S100A10 expression (C and D; note the clustered appearance of recycling endosomes in both YFP-S100A10–expressing and –nonexpressing cells). In contrast, recycling endosome clustering induced by annexin 2/S100A10 down-regulation was reversed by PMNanx2-GFP, which encodes amino acids 1–27 of human annexin 2 fused to GFP (E and F; note the nonclustered appearance of internalized TxTf in the two cells expressing PMNanx2-GFP). Expression of the PMNanx2-GFP construct in S100A10 siRNA-treated cells did not result in a significant reversion of the recycling ensdosome clustering (G and H). Dotted lines indicate position of depleted cells, arrowheads point toward the respective transferrin-positive recycling compartments. Bars, 10 μm.

Figure 6 (cont). transferrin receptor-positive structures (5-nm gold) often formed highly bent tubules of almost circular shape (D), not seen in control cells (C). They also contained an increased number of endosomal buds heavily decorated with clathrin antibodies (F). Counting of clathrin and TfR immunogold label in nine representative areas selected from three individual micrographs revealed a ratio (clathrin:TfR) of 1:7 in control cells and 1:2 in the depleted cells. Bars, 0.2 μm. The enlarged insets show a twofold magnification of the boxed regions.

GFP (for p11 minus N-terminal annexin 2). Annexin 2/S100A10-depleted cells were transfected with PMNanx2 and then fed with TxTf in the pulse-chase regime to visualize potential effects on recycling endosomes. Although the characteristic clustering of internalized transferrin was seen in the depleted cells, expression of PMNanx2 restored the transferrin pattern seen in unperturbed control cells, i.e., recycling vesicles dispersed throughout the cells containing TxTf on its way back to the plasma membrane (Figure 7, E and F). A corresponding rescue experiment using PMNanx2 was also carried out in S100A10 siRNA-treated cells. Here, no or only a minor rescue of the depletion phenotype, i.e., the perinuclear clustering of recycling endosomes was observed (Figure 7, G and H). Thus, expression of the N-terminal endosome binding site of annexin 2 rescues the defect in recycling endosome positioning seen in cells depleted of the annexin 2/S100A10 complex but not in those only depleted of S100A10.

DISCUSSION

For several annexins, endosomes have been identified as target membranes, and annexin 2, in particular, has been proposed to function in the endocytic pathway (Gerke and Moss, 2002). However, experiments supporting this view have relied so far on cell free systems or the overexpression of annexin mutant proteins and the effects on endocytic processes and/or endosome organization of a specific down-regulation of a given annexin have not been analyzed. We therefore used the RNA interference approach to elucidate whether annexin 2 as monomer or complexed with S100A10 is required for endosome dynamics in live cells. Transfection of HeLa cells with annexin 2-specific siRNA reduced the annexin 2 protein content to a low level but did not cause a reduction in the expression of annexin 1, the closest homolog of annexin 2 within the annexin family. Some persisting annexin 2 signals can be visualized at the plasma membrane of siRNA-treated cells by using the polyclonal anti-annexin 2 antibody msa419 that in contrast to the monoclonal antibody HH7 also recognizes the annexin 2/S100A10 heterotetramer. This residual annexin 2 colocalizes with S100A10, suggesting that it is most likely present in the heterotetrameric state. When associated with the plasma membrane, the annexin 2/S100A10 heterotetramer is tightly incorporated into the cortical cytoskeleton (Thiel *et al*., 1992) and has a longer metabolic half-life than the cytosolic pool (Zokas and Glenney, 1987). Such higher metabolic stability could explain that the plasma membrane-associated annexin 2/S100A10 complex is not efficiently down-regulated in the transient siRNA approach. Our siRNA data also support the view that complex formation increases the stability of the S100A10 subunit. It had been shown that annexin 2 overexpression caused an increase in S100A10 protein levels due to increased stability of the S100A10 protein via formation of the heterotetrameric complex (Puisieux *et al*., 1996). This indicates that the half-life of S100A10 critically depends on the presence of annexin 2 and explains the lower levels of S100A10 observed in annexin 2 down-regulated cells. Noncomplexed, monomeric annexin 2, on the other hand, is more stable as revealed by the unchanged annexin 2 levels in cells depleted of S100A10 by the siRNA approach. Thus, by targeting individually the two subunits of the annexin 2/S100A10 complex, we were able to generate cells either depleted of the entire complex (by annexin 2 siRNA treatment) or of the S100A10 subunit alone (by S100A10 siRNA).

Our analysis of endosomal pathways in the annexin 2/S100A10- or S100A10-down-regulated cells showed in both cases a specific perturbation in the recycling of transferrin that accumulated in perinuclear rab11-positive structures, most likely resembling recycling endosomes. A closer examination of these recycling endosomes by using whole-mount immunoelectron microscopy revealed a much more condensed appearance, a higher degree of tubular bending, and an increase in the number of endosome-associated buds that labeled heavily for clathrin. These buds most likely resemble those that have been proposed to serve as an exit pathway for recycling transferrin receptors (Stoorvogel *et al*., 1996). Interestingly, annexin 2 has previously been found associated with such buds, suggesting a possible role in proper bud positioning or formation (Zeuschner *et al*., 2001). Despite the marked alteration in ultrastructure and positioning of recycling endosomes, down-regulation of annexin 2 and S100A10 had no significant effect on any of the endosomal trafficking steps analyzed here. Only the recycling of internalized transferrin showed a minor reduction (~5%) in cells depleted of annexin 2/S100A10. Although this difference is at the limit of statistical significance, it has been observed consistently in all of our experiments. Possibly, it reflects a somewhat slower passage of internalized transferrin through the recycling compartment, which is aberrantly positioned in the depleted cells. Recent studies on transferrin recycling suggest that only a fraction of transferrin recycles through the recycling endosomes (slow pathway), whereas a major part of internalized transferrin takes a fast recycling route from sorting endosomes directly back to the plasma membrane (Sheff *et al*., 1999). Although the slower pathway is inhibited by a dominant-negative dynamin mutant, the direct route that bypasses recycling endosomes seems to depend on PI 3-kinase and is inhibited by wortmannin (van Dam and Stoorvogel, 2002). However, even the wortmannin-insensitive recycling pathway is not significantly reduced by the perinuclear clustering of recycling endosomes in our annexin 2/S100A10-depleted cells. Moreover, transferrin present in these perinuclear clusters is not blocked from leaving the cell as revealed by following the distribution of internalized transferrin in pulse-chase experiments involving longer times of up to 60 min (our unpublished data). Thus the clustering of recycling endosomes only has a minor effect on the passage of transferrin through the aberrantly positioned organelle and/or induces compensatory recycling routes, which, however, are not wortmannin sensitive.

The observation that a marked alteration in the distribution and/or ultrastructure of endosomes only has a minor effect on recycling rates is not without precedent. Microsurgical generation of cytoplasts without perinuclear endosomes, for example, does not block transferrin from recycling through morphologically different but rab11-positive endosomes (Sheff *et al*., 2002). Also, in RBL cells treated with antisense cDNA to down-regulate synaptotagmin III, internalized transferrin is not found in perinuclear recycling endosomes but recycling rates are not affected (Grimberg *et al*., 2003). Another example is the overexpression of the dominant-negative clathrin Hub mutant in HeLa cells. In addition to reducing receptor-mediated endocytosis at the plasma membrane this mutant induces a perinuclear aggregation of EEA1-positive endosomes without affecting the kinetics of receptor recycling (Bennett *et al*., 2001). Altogether and in line with our experiments, these examples indicate that the intracellular positioning of early endo-

somes is not a rate-limiting step in the recycling of membrane receptors.

Targeting the two subunits of the annexin 2/S100A10 complex individually and using different constructs in specific rescue experiments allowed us to identify the annexin 2/S100A10 complex as the relevant unit required for proper positioning of recycling endosomes. Both subunits are crucial because monomeric annexin 2 alone (in the S100A10 siRNA-treated cells) is not sufficient to keep the recycling endosomes from clustering and because S100A10 alone is not capable of reversing the clustering induced by annexin 2/S100A10 depletion in the annexin 2 siRNA-treated cells. Given the biochemical properties of the annexin 2/S100A10 complex, in particular its capability of forming highly organized structures on biological membranes (Lambert *et al*., 1997), it is tempting to speculate that the complex participates in stabilizing and/or regulating the shape of tubular recycling endosomes. Such organization could affect the formation and proper clathrin coating of endosomal buds required as specific exit sites for recycling receptors. A perturbation of this organization after annexin 2/S100A10 down-regulation could result in condensed endosomes, aberrantly bent tubules, and an altered clathrin decoration on endosomal buds, effects observed in the ultrastructural analysis of the depleted cells. Most likely, the Ca^{2+}-insensitive endosome binding site present in the N-terminal domain of annexin 2 is essential for a structural role of the annexin 2/S100A10 complex on tubular recycling endosomes. In the PMNanx2-GFP fusion construct this N-terminal site is capable of conferring proper recycling endosome distribution to annexin 2/S100A10-depleted cells. This activity is not retained in monomeric annexin 2, which is not able to maintain proper endosome distribution in S100A10 down-regulated cells. On the other hand, PMNanx2 is not capable of reversing the recycling endosome clustering in S100A10-depleted cells, indicating that the monomeric annexin 2 remaining in the S100A10 down-regulated cells is able to interfere with the PMNanx2 action. Thus, and in line with previous experiments (Jost *et al*., 1997), it seems that the N-terminal endosome binding site is only accessible for interaction in S100-complexed annexin 2 and the PMNanx2 mutant construct and not to the same extent in monomeric annexin 2. Nonetheless, monomeric annexin 2 could perhaps bind to endosomal membranes by some other means (possibly through its core domain), which does not allow to maintain the proper positioning of recycling endosomes but interferes with PMNanx2 binding. Future experiments establishing, for example, high resolution structural images of annexin 2/S100A10 bound to membranes, should aid the construction of annexin 2/S100A10 mutants not capable of forming organized structures on endosomes. Overexpression of such mutants should result in dominant-negative phenotypes and thereby provide a detailed structural explanation for the function of annexin 2/S100A10 in endosome positioning and organization.

ACKNOWLEDGMENTS

We thank Judith Klumperman and Willem Stoorvogel for stimulating discussions. We also thank R. Scriwanek and M. van Perski for excellent preparation of the electron micrographs and E. Ungewickell for supplying the clathrin antibody. This work was supported by a grant from the Deutsche Forschungsgemeinschaft (Ge 514/4-3 and SFB 629).

REFERENCES

Aniento, F., Gu, F., Parton, R.G., and Gruenberg, J. (1996). An endosomal beta COP is involved in the pH-dependent formation of transport vesicles destined for late endosomes. J. Cell Biol. *133*, 29–41.

Babiychuk, E.B., and Draeger, A. (2000). Annexins in cell membrane dynamics. Ca(2+)-regulated association of lipid microdomains. J. Cell Biol. *150*, 1113–1124.

Bennett, E.M., Lin, S.X., Towler, M.C., Maxfield, F.R., and Brodsky, F.M. (2001). Clathrin hub expression affects early endosome distribution with minimal impact on receptor sorting and recycling. Mol. Biol. Cell *12*, 2790–2799.

Daro, E., van der Sluijs, P., Galli, T., and Mellman, I. (1996). Rab4 and cellubrevin define different early endosome populations on the pathway of transferrin receptor recycling. Proc. Natl. Acad. Sci. USA *93*, 9559–9564.

Drust, D.S., and Creutz, C.E. (1988). Aggregation of chromaffin granules by calpactin at micromolar levels of calcium. Nature *331*, 88–91.

Emans, N., Gorvel, J.P., Walter, C., Gerke, V., Kellner, R., Griffiths, G., and Gruenberg, J. (1993). Annexin II is a major component of fusogenic endosomal vesicles. J. Cell Biol. *120*, 1357–1369.

Gerke, V., and Moss, S.E. (2002). Annexins: from structure to function. Physiol. Rev. *82*, 331–371.

Gerke, V., and Weber, K. (1984). Identity of p36K phosphorylated upon Rous sarcoma virus transformation with a protein purified from brush borders; calcium-dependent binding to non-erythroid spectrin and F-actin. EMBO J. *3*, 227–233.

Gorvel, J.P., Chavrier, P., Zerial, M., and Gruenberg, J. (1991). rab5 controls early endosome fusion in vitro. Cell *64*, 915–925.

Grimberg, E., Peng, Z., Hammel, I., and Sagi-Eisenberg, R. (2003). Synaptotagmin III is a critical factor for the formation of the perinuclear endocytic recycling compartment and determination of secretory granules size. J. Cell Sci. *116*, 145–154.

Gruenberg, J., and Maxfield, F.R. (1995). Membrane transport in the endocytic pathway. Curr. Opin. Cell Biol. *7*, 552–563.

Harder, T., and Gerke, V. (1993). The subcellular distribution of early endosomes is affected by the annexin II2p11(2) complex. J. Cell Biol. *123*, 1119–1132.

Hopkins, C.R., Gibson, A., Shipman, M., Strickland, D.K., and Trowbridge, I.S. (1994). In migrating fibroblasts, recycling receptors are concentrated in narrow tubules in the pericentriolar area, and then routed to the plasma membrane of the leading lamella. J. Cell Biol. *125*, 1265–1274.

Johnsson, N., Marriott, G., and Weber, K. (1988). p36, the major cytoplasmic substrate of src tyrosine protein kinase, binds to its p11 regulatory subunit via a short amino-terminal amphiphatic helix. EMBO J. *7*, 2435–2442.

Jost, M., Zeuschner, D., Seemann, J., Weber, K., and Gerke, V. (1997). Identification and characterization of a novel type of annexin-membrane interaction: Ca2+ is not required for the association of annexin II with early endosomes. J. Cell Sci. *110*, 221–228.

Kamal, A., Ying, Y., and Anderson, R.G. (1998). Annexin VI-mediated loss of spectrin during coated pit budding is coupled to delivery of LDL to lysosomes. J. Cell Biol. *142*, 937–947.

Lafont, F., Lecat, S., Verkade, P., and Simons, K. (1998). Annexin XIIIb associates with lipid microdomains to function in apical delivery. J. Cell Biol. *142*, 1413–1427.

Lambert, O., Gerke, V., Bader, M.F., Porte, F., and Brisson, A. (1997). Structural analysis of junctions formed between lipid membranes and several annexins by cryo-electron microscopy. J. Mol. Biol. *272*, 42–55.

Mellman, I. (1996). Endocytosis and molecular sorting. Annu. Rev. Cell Dev. Biol. 12575–12625.

Osborn, M., Johnsson, N., Wehland, J., and Weber, K. (1988). The submembranous location of p11 and its interaction with the p36 substrate of pp60 src kinase in situ. Exp. Cell Res. *175*, 81–96.

Powell, M.A., and Glenney, J.R. (1987). Regulation of calpactin I phospholipid binding by calpactin I light-chain binding and phosphorylation by p60v-src. Biochem J. *247*, 321–328.

Puisieux, A., Ji, J., and Ozturk, M. (1996). Annexin II up-regulates cellular levels of p11 protein by a post-translational mechanisms. Biochem J. *313*, 51–55.

Ren, M., Xu, G., Zeng, J., De Lemos Chiarandini, C., Adesnik, M., and Sabatini, D.D. (1998). Hydrolysis of GTP on rab11 is required for the direct delivery of transferrin from the pericentriolar recycling compartment to the

cell surface but not from sorting endosomes. Proc. Natl. Acad. Sci. USA *95*, 6187–6192.

Seemann, J., Weber, K., Osborn, M., Parton, R.G., and Gerke, V. (1996). The association of annexin I with early endosomes is regulated by Ca2+ and requires an intact N-terminal domain. Mol. Biol. Cell *7*, 1359–1374.

Sheff, D., Pelletier, L., O'Connell, C.B., Warren, G., and Mellman, I. (2002). Transferrin receptor recycling in the absence of perinuclear recycling endosomes. J. Cell Biol. *156*, 797–804.

Sheff, D.R., Daro, E.A., Hull, M., Mellman, I., Ren, M., Xu, G., Zeng, J., De Lemos Chiarandini, C., Adesnik, M., and Sabatini, D.D. (1999). The receptor recycling pathway contains two distinct populations of early endosomes with different sorting functions. J. Cell Biol. *145*, 123–139.

Sonnichsen, B., De Renzis, S., Nielsen, E., Rietdorf, J., and Zerial, M. (2000). Distinct membrane domains on endosomes in the recycling pathway visualized by multicolor imaging of Rab4, Rab5, and Rab11. J. Cell Biol. *149*, 901–914.

Stoorvogel, W., Geuze, H.J., Griffith, J.M., and Strous, G.J. (1988). The pathways of endocytosed transferrin and secretory protein are connected in the trans-Golgi reticulum. J. Cell Biol. *106*, 1821–1829.

Stoorvogel, W., Oorschot, V., and Geuze, H.J. (1996). A novel class of clathrin-coated vesicles budding from endosomes. J. Cell Biol. *132*, 21–33.

Thiel, C., Osborn, M., and Gerke, V. (1992). The tight association of the tyrosine kinase substrate annexin II with the submembranous cytoskeleton depends on intact p11- and Ca(2+)-binding sites. J. Cell Sci. *103*, 733–742.

Ullrich, O., Reinsch, S., Urbe, S., Zerial, M., and Parton, R.G. (1996). Rab11 regulates recycling through the pericentriolar recycling endosome. J. Cell Biol. *135*, 913–924.

van Dam, E.M., and Stoorvogel, W. (2002). Dynamin-dependent transferrin receptor recycling by endosome-derived clathrin-coated vesicles. Mol. Biol. Cell *13*, 169–182.

Zeuschner, D., Stoorvogel, W., and Gerke, V. (2001). Association of annexin 2 with recycling endosomes requires either calcium- or cholesterol-stabilized membrane domains. Eur. J. Cell Biol. *80*, 499–507.

Zobiack, N., Gerke, V., and Rescher, U. (2001). Complex formation and submembranous localization of annexin 2 and S100A10 in live HepG2 cells. FEBS Lett. *500*, 137–140.

Zokas, L., and Glenney, J.R., Jr. (1987). The calpactin light chain is tightly linked to the cytoskeletal form of calpactin I: studies using monoclonal antibodies to calpactin subunits. J. Cell Biol. *105*, 2111–2121.